Hindawi
Mobile Information Systems
Volume 2022, Article ID 3679898, 11 pages
https://doi.org/10.1155/2022/3679898

Research Article

Intelligent Online Monitoring Technology of Green Power Transmission and Transformation Equipment Based on Internet of Things

Junchao Li,[1] **Yuan Tian**,[2] **and Chen Zhang**[1]

[1]*Economic and Technological Research Institute of State Grid Ningxia Electric Power Co. Ltd., Yinchuan750002, Ningxia, China*
[2]*State Grid Ningxia Electric Power Co. Ltd., Yinchuan 750001, Ningxia, China*

Correspondence should be addressed to Junchao Li; 200631580144@whu.edu.cn

Received 26 February 2022; Revised 9 April 2022; Accepted 6 May 2022; Published 7 June 2022

Academic Editor: Chia-Huei Wu

To address the problems of insufficient real-time monitoring data, insufficient accuracy, and low reliability of current power grid monitoring systems, we offer intelligent online monitoring technology research of green energy transmission and conversion devices based on Internet technology. The sensor tag is integrated with various electrical equipment status monitoring sensors, so that the electrical equipment status acquisition terminal has the ability of recognition and perception. Firstly, the propagation characteristics of electromagnetic wave in substation are analyzed, and the propagation path loss model of electromagnetic wave is established. Secondly, a multiantenna RFID system is proposed to solve the problem of electromagnetic wave multipath effect. Moreover, the communication channel model of substation multiantenna (radio frequency identification, RFID) monitoring system is established, the factors affecting the performance of substation multiantenna RFID system are analyzed, and the precautions for the installation of multiantenna RFID system are put forward. A new anticollision algorithm is proposed compared to the traditional algorithm, based on the interference of collisions between the sensor markings of the multiantenna RFID control system in the substation. The results show that as the number of sensor markings increases, the total duration of the enhanced adaptive time slot and multitree search collision (improved adaptive time slot and multitree search anticollision, IATMSA) algorithm is always less than that of the IAMS algorithm and the square algorithm, basically maintained at 50% to 60%, up to about 75%. In the improved adaptive multitree search (improved adaptive multitree search, IAMS) anticollision algorithm, the IAMS algorithm determines the choice by calculating the size of the collision factor. The binary tree algorithm is basically about 45%, and the quadtree algorithm is basically about 30%. Figure shows the online monitoring technology for power transmission and conversion devices based on Internet of Things technology.

1. Introduction

With the development of the 21st century, a new round of energy revolution centered on power production is developing faster and faster, and the power grid is facing more and more challenges in the process of development. In order to promote the continuous development of power industry, the power grid technology needs to carry out corresponding technological transformation and development according to the development of society, further promote the innovation of power grid technology, and optimize the allocation of energy. With more and more types of power grid required to be connected, the scale of power grid needs to be gradually expanded to meet the current social needs [1]. Different kinds of energy need distributed access, and the identity of power users needs to be accurately located to further improve the reliability and economy of the power grid. The development of power grid also includes many deficiencies: the transmission of energy and the access and exit of power supply [2]. In terms of vertical performance, the response speed of the mechanism is slow, which is difficult to effectively meet the different needs of multiple users. Because there are different information islands in each information system, there are deficiencies in resource sharing within the information system, and there are isolated and independent parts in the system, which is difficult to form an effective and

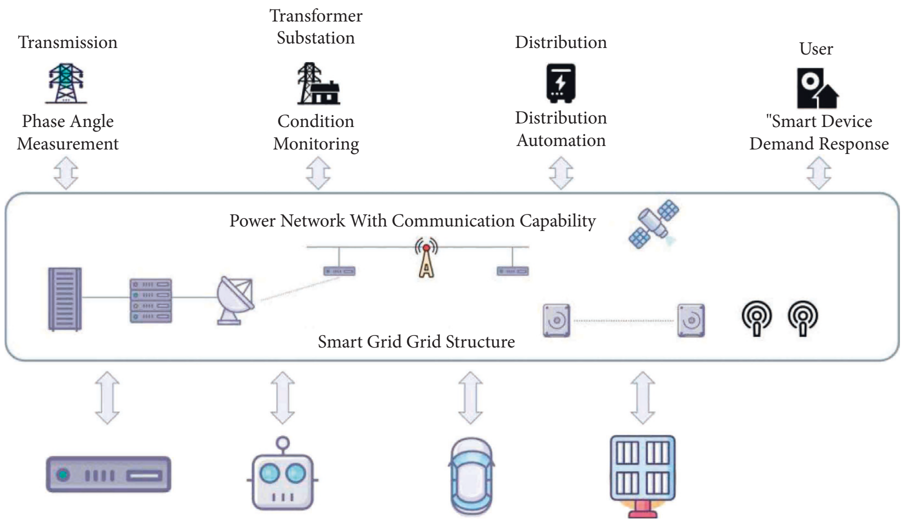

Figure 1: Online monitoring technology of power transmission and transformation equipment based on Internet of Things technology.

unified organic whole. Among them, due to the low degree of intelligent optimization of the overall power grid, it is also necessary to establish a perfect organic whole and further optimize the intelligent power grid [3]. Combined with the definition of transmission network, it can be found that the realization of China's strong smart grid is based on a strong physical power grid, which takes the information platform as the support, makes a unified and overall analysis in combination with relevant control means, including other relevant links such as power production and transmission, and analyzes its business scope. Business division shall be carried out in multiple scopes and links such as production scheduling and production transportation, management shall be carried out in production scheduling, power grid construction, power trading, and other links in business, and the whole replacement process of power grid construction, and operation and maintenance shall be managed in the design and planning of the whole power grid. In the information management flow of the whole smart grid, the relevant levels are comprehensively analyzed through collection, transmission, and display, and the real-time information exchange of the shared grid is realized through the establishment of the network information platform and the horizontal and vertical communication [4]. The online monitoring technology of power transmission and transformation equipment based on Internet of Things technology is shown in Figure 1.

As the basis of condition-based maintenance, wireless monitoring of power transmission and transformation equipment needs to analyze the electrical and physical characteristics of electrical equipment by using information technology, sensor technology, computer technology, and other related technologies on the basis of uninterrupted power supply, and monitor the equipment continuously and periodically [5]. Finally, analyze and collect the information processing and relevant data and parameters, analyze the wireless evaluation status through such trend, analyze the remaining life of the equipment, judge the change trend and condition maintenance, find the faults in the equipment in advance, and provide alarm information when necessary [6]. Power transmission and conversion communication is an important link of smart grid. At present, China Electric Grid Corporation is carrying out a comprehensive maintenance of power transmission and conversion equipment, including relevant exploration and practice of equipment condition monitoring, evaluation, risk, and asset life cycle management. However, compared with the goal of state-based equipment maintenance and efficient operation and maintenance under the smart grid, there are still many problems, mainly including: (1) the power grid structure is still weak, the equipment level and health level of power transmission and transformation equipment still cannot meet the requirements of building a strong power grid, and the systematic equipment state evaluation has just started; (2) there is still a lack of intelligent means for equipment condition monitoring, the amount of online monitoring status of primary equipment is limited, the standards of condition monitoring devices from different manufacturers are not unified, and the communication means are still dominated by cables, which makes it difficult to connect in the substation and increases the maintenance workload; (3) there is still no effective method for the asset management used for equipment maintenance. The collection, return, and regular inspection of maintenance assets are still dominated by paper document management, which is inefficient, and cannot realize the data sharing of asset information. It is difficult to effectively control the phenomena of overdue inspection and missed inspection, resulting in potential safety hazards for equipment operation and maintenance. Radio frequency recognition technology, which is an intelligent object recognition and monitoring tool, and wireless sensor network technology, combined with wireless communication networks, provide new intelligent tools to correct the condition of power transmission and conversion devices [7].

2. Literature Review

There are some common problems in the electrical equipment condition monitoring system of power grid, such as insufficient data acquisition, incomplete information acquisition, and low system reliability [8]. He Z. et al. and others believe that the longer the history of power transmission and transformation research, the more developed the technology of insulation mechanical state of equipment, including equipment transformer, equipment switch, and equipment transformer [9]. Ding Y. et al. put forward the research points and system framework of building smart grid monitoring system based on Internet of Things technology in the context of smart grid and confirmed the feasibility of applying Internet of Things technology to smart grid monitoring system [10]. Zhao J. et al. studied and analyzed the information security technology of Internet of Things applied in smart grid, and put forward the protection system and security measures of Internet of Things information security system applied in smart grid [11]. Nazir and Shao studied and analyzed the wireless communication system of Internet of Things and proposed a wireless communication guarantee mechanism of Internet of Things for smart grid [12]. Nazir and Shao proposed to combine the Internet of Things and EPON technology to analyze the security system of the Internet of Things under the background that the Internet of Things is used in smart grid and based on the current situation and technical characteristics of power communication network resources, so as to provide premise guarantee for the wide application and construction of the Internet of Things in smart grid [12]. Saeed et al. and others constructed the transmission line condition monitoring system based on Internet of Things technology, PON technology, and fuzzy expert diagnosis technology. In terms of software, experiments verified the accuracy and enforceability of the system [13]. Mamouras and Wang conducted a feasibility study and analysis on the application of RFID technology with sensors in the status information acquisition of substation electrical equipment. The experimental verification shows that the RF tag should adopt the active tag, the communication distance should be between 50 and 150 m, and the obstacles should be avoided between the communication paths [14].

Based on this research, we offer a study of intelligent online monitoring technology for green energy transmission and conversion devices based on Internet of Things technology. Object information can be obtained anytime, anywhere, and object information can be transmitted to the actual destination. Analyze and process time, accuracy, and huge amounts of information and data through the enterprise's private network or operator network, and implement intelligent object processing.

3. Research Methods

3.1. State Monitoring of Power Transmission and Transformation Equipment and Key Technologies of Internet of Things

3.1.1. Technical Features of Internet of Things. As an important part of information technology, the Internet is a major development and change in the information industry [15]. The Internet of Things is narrowly defined as the "Internet of Things," while the Internet of Things is broadly defined as the integration of information space and physical space through information-sensing devices such as radios [16], frequency recognition, sensors, and global positioning systems. According to the agreed protocol, any object can be identified by a unique code through encoding technology, connected to the Internet to exchange information and create a network. Because of its ability to intelligently identify, locate, monitor, control, and manage, Internet technology has so far reached a high level in human society through the integrated use of information technology.

(1) Real-time information collection: a large number of different types of sensors are deployed on the Internet of Things, and these sensors collect the required information periodically at a specific frequency, so that the obtained data are in a state of dynamic change and continuous update, which is real time.

(2) Effective data transmission: the Internet remains the core of Internet of Things technology. Combining wired + wireless communication with the Internet allows for accurate transmission of object information in real time.

(3) Intelligent information processing: analyze and process the massive information obtained from sensors, and obtain useful data suitable for different fields and different users according to needs [17].

3.1.2. Basic Principle of Wireless Communication Channel Propagation of Monitoring System. ISM (industrial, scientific, and medical) frequency band generally does not need to apply for a license, and this frequency band can be used all over the world. Therefore, radio frequency identification (RFID) systems usually work in this frequency band. ISM frequency band includes 125 kHz, 13.56 MHz, 915 MHz, 2.45 GHz, and 5.8 GHz. RFID tag and reader usually use the combination method to realize the communication between signals. In the communication channel, the signal data exchange is completed through the timing relationship. There are generally two coupling modes: one is inductive coupling, including LF (125 kHz) and HF (13.56 MHz) RFID communication system; the other is electromagnetic backscattering, which is described by radar principle model according to the spatial propagation law of electromagnetic wave. For the substation equipment condition monitoring system, if the RFID communication system is applied to it, we must first ensure that the RFID communication system has sufficient communication identification path. Generally, the communication distance of equipment in the substation is within a few hundred meters. Because the communication distance of LF and HF frequency bands is generally within a few meters, it is not suitable for the condition monitoring system of electrical equipment in the substation. This paper adopts LF and HF band RFID system. Therefore, this paper only discusses the RFID communication system based on electromagnetic backscatter. In addition, the communication distance of passive RFID tags of electromagnetic backscatter type is generally within 1 m, which cannot ensure the effective communication distance of the electrical equipment condition monitoring system in the substation. Therefore, the power transmission and transformation of electrical equipment condition monitoring system adopt the sensor tag composed of active RFID tag and sensor fusion.

(1) Direct electromagnetic wave (free space propagation). The direct path of electromagnetic wave is free space propagation. Free space propagation is the most ideal case, and if the electromagnetic wave propagation mode is only direct path, the path loss is the smallest. At this time, the power relationship between reader and RFID tag is

$$P_{r\_\text{reader}} = \frac{P_{t\_\text{reader}} G_{t\_\text{reader}} G_{r\_\text{tag}} \lambda^2}{\left(4\pi L_0\right)^2}, \tag{1}$$

where P_{r_reader} is the transmitting power of the reader, P_{r_tag} is the transmitting gain of the reader, G_{t_reader} is the receiving gain of the tag, G_{r_tag} is the path length between the reader and the tag, and L_0 is the electromagnetic wavelength. According to formula (1), the received power of the tag is inversely proportional to the square of L_0; that is, with the increase of L_0, the received power will gradually decrease; the receiving power of electromagnetic waves with different frequencies is different. The higher the frequency, the smaller the wavelength and the smaller the receiving power. The logarithmic form of path loss in free space is

$$L\text{free}\,(dB) = -20\ \log\ 10\left(\frac{\lambda}{4\pi L_0}\right). \tag{2}$$

According to formula (2), the path loss in free space increases with the increase of L_0.

(2) Electromagnetic wave reflection. When the electromagnetic wave encounters objects larger than its own wavelength (ground, wall, substation line tower, etc.), it will be reflected. The field strength of reflected electromagnetic wave is affected by Fresnel reflection coefficient, which is a function of the material of the reflecting surface and is related to the incident angle, frequency, and polarization mode of electromagnetic wave. When the incident medium of electromagnetic wave is free space, the Fresnel reflection coefficient is shown in:

$$\Gamma_v = \frac{-\varepsilon_r \sin(\alpha) + \sqrt{\varepsilon_r - \cos^2(\alpha)}}{\varepsilon_r \sin(\alpha) + \sqrt{\varepsilon_r - \cos^2(\alpha)}}, \tag{3}$$

$$\Gamma_H = \frac{-\varepsilon_r \sin(\alpha) + \sqrt{\varepsilon_r - \cos^2(\alpha)}}{\varepsilon_r \sin(\alpha) + \sqrt{\varepsilon_r - \cos^2(\alpha)}}, \tag{4}$$

where Γ_v and Γ_H represent the reflection coefficient of vertically polarized electromagnetic wave and horizontally polarized electromagnetic wave, respectively, α is the angle between the incident electromagnetic wave and the horizontal plane when the electromagnetic wave is reflected, and ε_r is the relative dielectric constant of the electromagnetic wave reflecting surface. Table 1 shows the relative permittivity and conductivity of common materials [18].

Table 1: Common material coefficients.

Material science	Relative dielectric constant	Conductivity (S/m)
Rough ground	3	0.001
General ground	14	0.003
Smooth ground	24	0.002
Freshwater	70	0.001
Glass	3	0.001

For an ideal conductor, regardless of the incident angle, $\Gamma_H = 1$, $\Gamma_v = -1$. After the electromagnetic wave is reflected through the reflecting surface, the synthetic field strength is the vector sum of the electric field strength of the direct wave and the reflected wave, and all kinds of polarized waves can be regarded as the vector superposition of the vertical polarized wave and the horizontal polarized wave [19]. Therefore, when analyzing the propagation path loss of electromagnetic wave, it can be divided into vertical polarization wave and horizontal polarization wave. In the power transmission and transformation environment, due to the ubiquitous metal wall of the substation, when the electromagnetic wave propagates in the substation, it will continue to reflect on the metal wall, resulting in multipath effect, and the path loss will increase a lot compared with the free space loss. Therefore, when analyzing the performance of RFID sensor tag communication system, it is essential to consider the reflection path of electromagnetic wave in substation.

3.1.3. Propagation Characteristics of Wireless Communication Channel of Monitoring System. Affected by the propagation environment, the wireless channel will have direct, reflection, diffraction, scattering, and other propagation modes. When the electromagnetic wave reaches the receiving point in different ways, it will cause signal fading. Electromagnetic wave signal fading includes small-scale signal fading and large-scale signal fading. Small-scale signal fading is caused by multipath effect. Large-scale fading is related to communication distance and fading factor. The fading factor is generally determined by the environment.

(1) Large-scale fading. Large-scale signal fading represents the variation trend of distance field strength between signal transmitter and signal receiver, and the attenuation of average received power within a certain distance. Large-scale fading is mainly affected by the distance between transmitter and receiver and the surrounding terrain. The radiation of transmitting antenna and the propagation of wireless channel cause the phenomenon of electromagnetic wave path fading, resulting in path loss. Lognormal shadow fading model is a common model for large-scale fading. This statistical model is discussed in detail below. Lognormal shadow model is shown in

$$Pl(L) = Pl(L_0) + 10A\ \log\left(\frac{L}{L_0}\right) + X_\alpha, \tag{5}$$

where $Pl(L)$ represents normal shadow path loss, $Pl(L_0)$ represents reference value, X_α represents normal random variable with standard deviation of a, and A represents path fading loss coefficient. Some researchers have summarized the parameters of normal shadow model in some common environments, as shown in Table 2.

The lognormal shadow model does not show the relationship between path loss and frequency. In the actual wireless RFID communication system, the path loss is affected by frequency, and the path loss model affected by frequency is (4):

$$\sqrt{Pl(f)}\infty f^{\delta}, \tag{6}$$

where δ is the frequency attenuation factor, generally between 0.8 and 1.4. The model has been used to estimate the relationship between path loss and frequency.

(2) Small-scale fading. Small-scale fading is that the signal propagates along two or more paths, causing the received signals to interfere with each other and causing signal fading. Multipath effect is a very complex process, which can be regarded as a random process in time and space. Small-scale fading is affected by multipath propagation, mobile station motion, signal bandwidth, surrounding objects, and other factors. Time dispersion, Doppler spread, coherent time, and coherent bandwidth are the parameters to measure the characteristics of small-scale fading. Doppler effect and coherence time characterize the time-varying characteristics of small-scale fading of system signals. Coherence bandwidth and time dispersion are the parameters to measure the time dispersion characteristics of small-scale fading.

If there is no line of sight propagation between reader and RFID tag, Rayleigh distribution can be used to characterize the signal fading amplitude of the system signal caused by electromagnetic wave multipath effect. The probability density function of Rayleigh distribution is (5):

$$f(x) = \begin{cases} \dfrac{x}{P}\exp\left(-\dfrac{x^2}{P}\right), x > 0, \\ 0, \end{cases} \tag{7}$$

where x is the amplitude envelope of the received signal and P is the parameter of Raleigh distribution.

If there is line of sight propagation between the reader and RFID tag, and the signal strength of the direct path is stronger than that of other paths, Rician distribution can be used to characterize the signal fading amplitude of the system signal caused by electromagnetic wave multipath effect. The probability density function of Rician distribution is (6):

$$f(x) = \begin{cases} \dfrac{x}{P}I_0\left(\dfrac{x\mu}{p}\right)\exp\left(-\dfrac{x^2+\mu^2}{2P}\right), x \geq 0, \\ 0, \end{cases} \tag{8}$$

$I_0(x)$ is the first kind of zero-order Bessel function, and the output is the amplitude value of sight distance component. The Rician probability distribution is shown in Figure 2.

Table 2: Model parameters under common environment.

Building	Frequency (MHz)	A	α
Retail store	803	2.1	7.6
Office hard partition	803	1.4	4.1
Office soft partition	1400	2.0	6.0
Indoor corridor	800	2.0	6.0

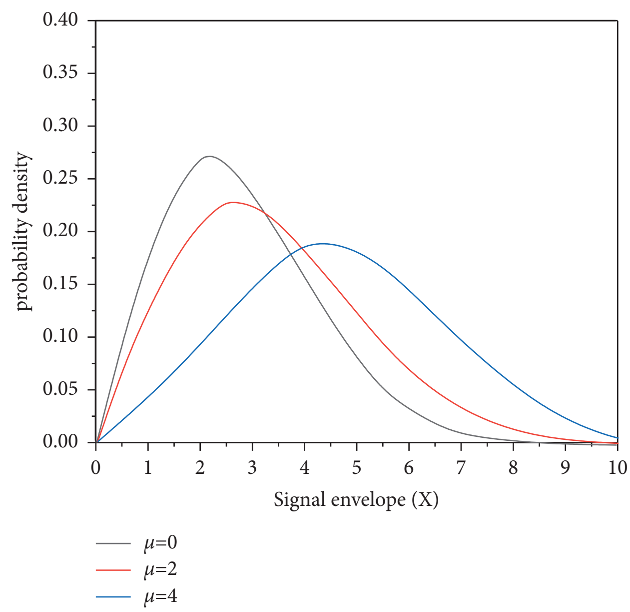

Figure 2: Rician probability distribution.

3.2. Electromagnetic Wave Propagation Loss Model

3.2.1. Free Space Loss of Electromagnetic Wave. When the electromagnetic waves of a substation control system propagate in free space, the path loss of the substation control system is related to the frequency of the electromagnetic wave, the distance between the reader and sensor markings, and the frequency change curve. Electromagnetic waves are shown in Figure 3. As shown in Figure 3, as the frequency of the electromagnetic wave leakage loss in the substation control system increases, the leakage loss increases as the L distance between the reader and the sensor cover increases [20, 21].

3.2.2. Reflection Loss of Electromagnetic Wave. In the substation monitoring system, electromagnetic wave will be reflected on the ground and metal wall due to the metal shielding effect of electrical equipment. Due to the different materials of reflective medium ground and metal wall, the reflection of electromagnetic wave will be very different. Therefore, in the study of electromagnetic wave propagation path loss of substation supervision side system, electromagnetic wave reflection loss is essential [22]. In the substation monitoring system, there are three reflected rays of the signal transmitted by the reader antenna: one is based on the ground as the reflecting surface, and the other two are based on the sides of two metal walls. In this paper, assuming that the path loss of electromagnetic wave with secondary

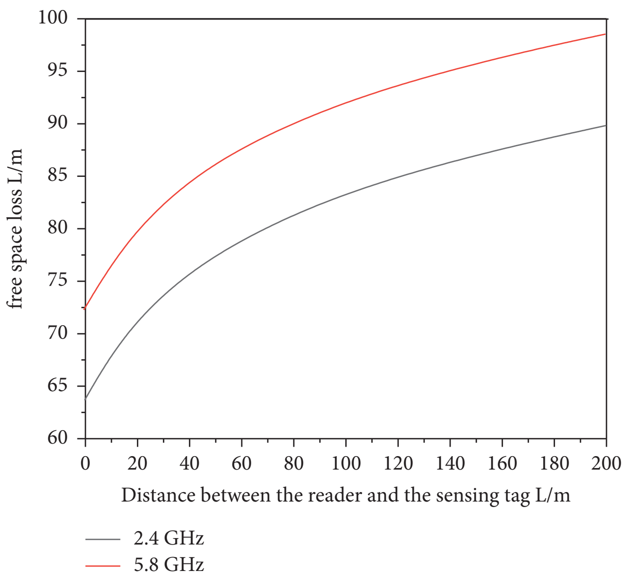

Figure 3: Free space path loss.

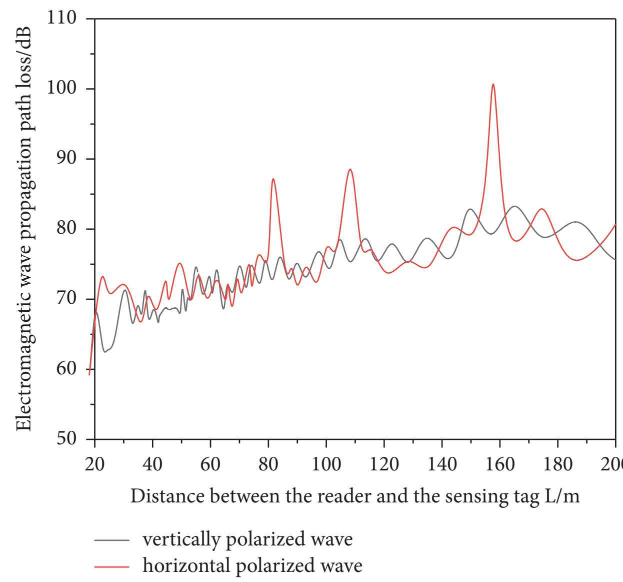

Figure 4: Path loss considering electromagnetic wave reflection.

reflection of electromagnetic wave is too large to reach the receiver, the reflection loss of electromagnetic wave in substation monitoring system is (7):

$$Lt\,(dB) = -20\ \log\ 10\left(\sum_{i=1}^{N}\Gamma_i\frac{2\pi}{\lambda}\Delta L_i\right), \tag{9}$$

where n is the number of reflected rays of electromagnetic wave in the substation monitoring system, $N = 3$, L_i is the path length of the first ray, ΔL_i is the path difference between the i-th ray path and the free space path L_0, and Γ_i is the reflection coefficient of the first ray. Considering the free space loss and electromagnetic wave reflection loss, the electromagnetic wave loss of substation monitoring system is (8):

$$PLs\,(dB) = -20\ \log\ 10\left(\frac{\lambda}{4\pi}\right) - 20\ \log\ 10\left(\frac{1}{L_0} + \sum_{i=1}^{N}\Gamma_i\frac{(2\pi/\lambda)\Delta L_i}{L_i}\right). \tag{10}$$

The electromagnetic wave propagation path loss considering free space loss and reflection loss in the substation monitoring system can be obtained from formula (13), and the variation trend of electromagnetic wave propagation path loss is shown in Figure 4. It can be seen from Figure 4 that the electromagnetic wave reflection and path loss in free space considered in the substation monitoring system are related to the electromagnetic wave polarization mode. Different polarization modes vary with the distance between the reader and the sensing label. In the first 100 m or so, the attenuation trend of electromagnetic wave propagation path loss is close, which shows that the electromagnetic wave multipath effect is more obvious in this distance in the substation monitoring system. With the increase of the distance L between the reader and the sensor tag, the path loss degree of small-scale fading caused by multipath effect decreases and the large-scale fading effect increases [23, 24].

3.3. Multiantenna RFID System

3.3.1. Multiantenna RFID System Channel Model. According to the analysis of electromagnetic wave propagation path loss, the channel shock response of electromagnetic wave based on ray tracing propagation is

$$g\,(t) = \sum_{i=1}^{N} R_i\delta\,(t-\tau_i)\exp\,(-j\varphi_i), \tag{11}$$

where $g\,(T)$ is the ray tracing response. If the line of sight propagation ray amplitude is 1, R_i is the amplitude of the i-th ray, that is, formula

$$R_i = \Gamma_i, \tag{12}$$

τ_i is the time delay of the first ray, i.e.,

$$\tau_i = \frac{L_i}{c}, \tag{13}$$

C is the speed of light. φ_i is the phase of the first ray, i.e.,

$$\varphi_i = \frac{L_i}{\lambda}\mathrm{mod}2\pi. \tag{14}$$

Change (17) into narrowband frequency response:

$$g\,(t) = \sum_{i=1}^{N} R_i\exp\,(-j\varphi_i)\exp\,(-j2\pi f\tau_i). \tag{15}$$

The electromagnetic wave propagation loss model is established based on the ray tracing method of tent law, and the channel between each transmitting antenna and receiving antenna is given. Then, it is extended to multiple input and multiple output channel matrix. (9) can be rewritten into (14):

$$h_{ij}\,(t) = \sum_{i=1}^{N} R_n\exp\left(-j\frac{2\pi Ln}{\lambda}\right)\exp\,(-j\varphi_n), \tag{16}$$

If line of sight propagation is considered (15),

$$h_{ij}(t) = \sum_{i=0}^{N} R_n \exp\left(-j\frac{2\pi Ln}{\lambda}\right)\exp\left(-j\varphi_n\right), \quad (17)$$

where $h_{ij}(t)$ is the channel response between the i-th transmitting antenna and the j-th receiving antenna.

3.3.2. Performance Analysis of Multiantenna RFID System. In a multiantenna RFID control system, the system device has a definite effect on the bit depending on the height of the reader installation, the height of the sensor label installation, the number of antennas, the location of the antenna, and other factors. According to the bit error rate of multiantenna RFID control system, the performance of antenna RFID control system is analyzed. During system performance analysis, the MATLAB cftool toolbox is used to simulate channel design data (see Table 3) and the effect of various parameter changes on the performance of the substation's multiantenna RFID control system; the relationship between the system bit error rate and the reader recognition distance is used to evaluate system performance.

Performance analysis of single antenna and multiantenna RFID systems: in the substation, due to the metal shielding effect, the multipath effect will be generated in the communication process between the sensor tag and the reader, which may cause the sensor tag to not receive the effective activation signal or the reader to not successfully read the backscatter signal of the sensor tag. Therefore, this paper uses the method of using multiple transceiver antennas to solve this problem. The performance comparison between the systems using multitransceiver antenna RFID and the original single-antenna RFID system is shown in Figure 5. As can be seen from Figure 5, after adopting the multiantenna RFID system, the bit error rate of the system is significantly improved, and the more antennas are adopted; the smaller the bit error rate of the system, the better the performance of the system. In addition, in the substation environment, if the reader recognition distance can reach more than 150 m, changing the number of reader receiving antennas has no obvious effect on improving the bit error rate of the system. Therefore, the performance of the system should be improved from other parameters [25].

The influence of reader antenna height on system performance: the substation environment is complex and changeable. When the multiantenna RFID system is applied to the substation, the influence of the installation height of the reader antenna on the system performance cannot be ignored. Different reader antenna heights will produce different effects, which will directly affect the strength of the received signal of the system. Figure 6 shows the relationship between the bit error rate of a multiantenna RFID control system and the height of the reader antenna. As can be seen in Figure 6, the higher the height of the reader antenna, the lower the bit rate error of the system, i.e., the better the system performance. An increase in the height of the reader antenna will reduce the system channel path loss, weaken the signal interference caused by the multipath effect, and

Table 3: Simulation and experimental model parameters.

Parameter	Numerical value
Reader height	10 m
Sensor label height	5 m
Frequency	2.2 GHz
Metal wall spacing	15 m
Distance from reader to metal wall	10 m
Sensing label to metal wall	10 m
Path loss factor	1 m
Transmitting power of reader antenna	22 dBm
Tag scattering signal power ratio	0.77
Reader transceiver antenna gain	5 dBi

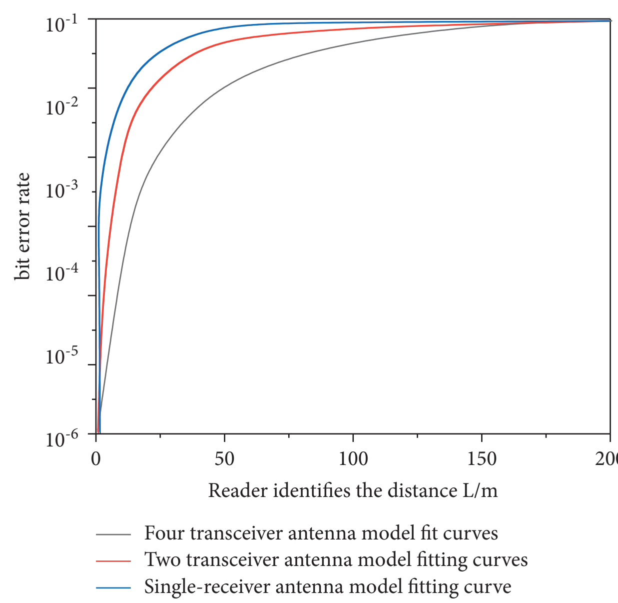

Figure 5: Effect of antenna number on system performance.

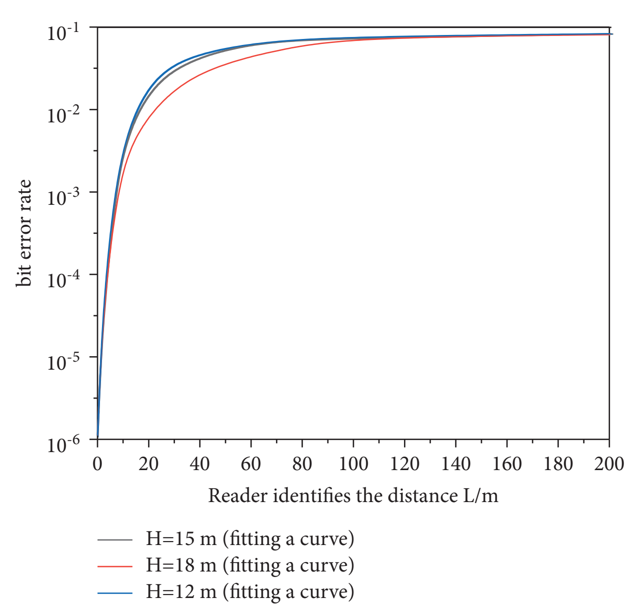

Figure 6: Effect of height on reader system performance.

increase the useful signal strength in the signal received by the system, and the bit error rate will decrease accordingly.

The influence of antenna polarization mode on system performance: different polarization modes of antenna will cause different propagation path losses of electromagnetic wave in the system channel and make the interference degree of multipath effect on the received signal different. Therefore, it is essential to study and analyze the impact of antenna polarization mode on the performance of substation multiantenna RFID monitoring system. The influence of different polarization modes on the system bit error rate is shown in Figure 7. It can be seen from Figure 7 that in the substation multiantenna RFID monitoring system, the antenna polarization mode has little impact on the bit error rate of the system, and the horizontal polarization mode is better than the vertical polarization mode. Therefore, for the substation multiantenna RFID monitoring system, the horizontal polarization effect of the antenna is better.

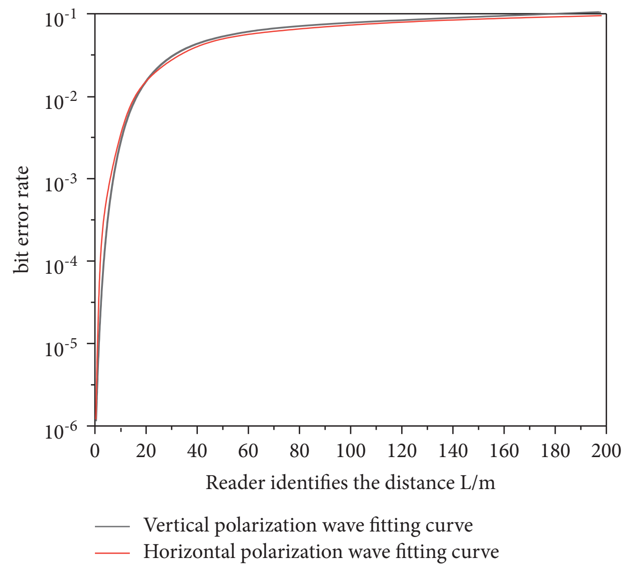

Figure 7: Influence of antenna polarization mode on system performance.

4. Result Discussion

4.1. Description of Anticollision Algorithm of Multiantenna RFID Monitoring System

4.1.1. IAMS Algorithm. IAMS algorithm selects binary tree or quadtree algorithm by calculating the size of collision factor μ_0, optimizes the reader prefix, and defines collision factor $\mu_0 = r_c/r = r[1 - (0.5)^{n-1}]/r = 1 - (0.5)^{n-1}$. r is the length of sensor tag ID code, r_c is the number of collision bits, and n is the total number of sensor tags. In IAMS algorithm, $n = 3$ is taken as the critical value of binary tree algorithm and quadtree algorithm to obtain the collision factor $\mu_0 = 1 - (0.5)^{3-1} = 0.75$. When $\mu_0 < 0.75$, the binary tree algorithm is adopted, and the reader generates two prefixes according to one collision bit. Otherwise, the quadtree algorithm is adopted, and the reader requires the tag to return the high two-bit collision prefix information. The IAMS algorithm is applied to the substation multiantenna RFID monitoring system. The simulation results show that the recognition speed and throughput of the algorithm cannot meet the requirements of the system. Therefore, this article proposes an improved IATMSA algorithm against collisions that combines adaptation time and multiple trees.

4.1.2. IATMSA Algorithm. Because the sensor tag of the multiantenna RFID monitoring system of electrical equipment selects the active tag, when the sensor tag measures the corresponding parameters of electrical equipment, the sensor tag will first send the application identification command to the base station reader, and then the reader will read the sensor tag information after the reader responds. Based on the above special environment, an IATMSA algorithm is proposed on the basis of IAMS algorithm.

First, the principle of priority allocation of dedicated time slots is formulated. The difference between the sensor tag and the traditional tag communication system is that the sensor tag has two communication channels: one is the sensor communication channel of wireless sensor network, and the other is the tag RF communication channel. After the sensor tag collects the status information of electrical equipment, the active sensor tag first sends the reading information instruction to the reader successively, and the special time slot is allocated based on the order of sending instructions of the active sensor tag. If only one sensor tag sends an identification instruction at a certain time, after the base station unit confirms the instruction through verification, the reader assigns a dedicated time slot to the sensor tag, so as to successfully obtain the electrical equipment status information perceived by the sensor tag. After the exclusive time slot is allocated, other sensing tags have no right to use the time slot. Secondly, when the sensor tag sends the application command to the reader, the sensor tag will collide; that is, two or more sensor tags send the application command at the same time. For the sensor tag applied for collision, the base station determines the number of sensor tag collisions through model calculation. Finally, the IAMS algorithm is used to identify the applied label. IATMSA algorithm steps are as follows:

Step 1: The sensor tag sends an application command and assigns a dedicated time slot to the sensor tag according to the principle of priority application and priority allocation of dedicated time slot.

Step 2: Judge whether there is an applied collision. If there is no collision, successfully read the sensing label. If there is a collision, proceed to the next step.

Step 3: Determine the number of collision sensor tags and calculate the collision factor μ_0. If $\mu_0 < 0.75$, use the binary tree algorithm; otherwise, the quadtree algorithm is used.

Step 4: Judge whether the stack is empty. If it is empty, it ends; otherwise, skip to step 3.

4.1.3. Algorithm Performance Index. In this paper, the performance of IATMSA algorithm is analyzed by calculating the total number of time slots and throughput. Because in the electrical equipment condition monitoring system, the sensor tag successively sends the application recognition command to the reader; there will be two situations: application success and application collision. For successfully applied sensor tags, the total number of time slots is the number of successfully applied sensor tags n_1, because these sensor tags do not have collision time slots. However, the sensor tag applying for collision needs to be identified by IAMS algorithm, so the total number of time slots of the sensor tag applying for collision is

$$T(n_2) = \sum_{i=0}^{k} 4^i + \frac{5}{3}n_2 - \left[1.16n_2 - 4^{k+1}\left(1 - 4^{-(k+1)}\right)^{n_2}\right] + \left\{0.72n_2 - 4^{k+1}\left[1 - \left(1 - 4^{-(k+1)}\right)^{n_2} - \frac{n_2}{4^{k+1}}\left(1 - 4^{-(k+1)}\right)^{n_2 - 1}\right]\right\}, \tag{18}$$

where n_2 is the number of sensing tags applying for collision and k is the search depth, $k = \log_4 (n_2/3)$.

According to the above analysis, if the number of sensor tags applying for collision can be determined, the total number of time slots of IATMSA algorithm can be determined. It is assumed that within t time, all sensor tags send the application identification command, and the number of all sensor tags is n. Since there are only two situations of applying for collision time slot and applying for successful time slot within t time, the probability of applying for collision time slot and applying for successful time slot is 1/2, respectively. The expectation of calculating the number of applied collision sensor tags according to the arrangement and combination is (17):

$$\mathrm{E}(n) = \sum_{m=0}^{n} C_n^m m\left(\frac{1}{2}\right)^m \left(1 - \frac{1}{2}\right)^{n-m}. \tag{19}$$

In equation (19), n is the number of all sensing tags and m is the number of collision slot tags. The number of applied collision sensing tags calculated in the formula is expected to be used as n_2 in formula (16) to calculate the total number of applied collision time slots. Then, the total number of time slots of all sensing labels is

$$T(n) = n_1 + T(n_2). \tag{20}$$

The number of time slots of collision tracking tree algorithm and the total number of time slots approximated by linear fitting of quadtree algorithm are (19) and (20), respectively:

$$t_{\text{rock}} = 2n - 1, \tag{21}$$

$$t(n) \approx 2.88n. \tag{22}$$

The binary tree algorithm can be deduced as

$$t_{BT}(n) = 1 + 2\sum_{k_0-0}^{\infty} 2^{k_0}\left[1 - \left(1 - 2^{-k_0}\right)^n - n * 2^{-k_0}\left(1 - 2^{-k_0}\right)^{n-1}\right], \tag{23}$$

where k_0 is the search depth of binary tree.

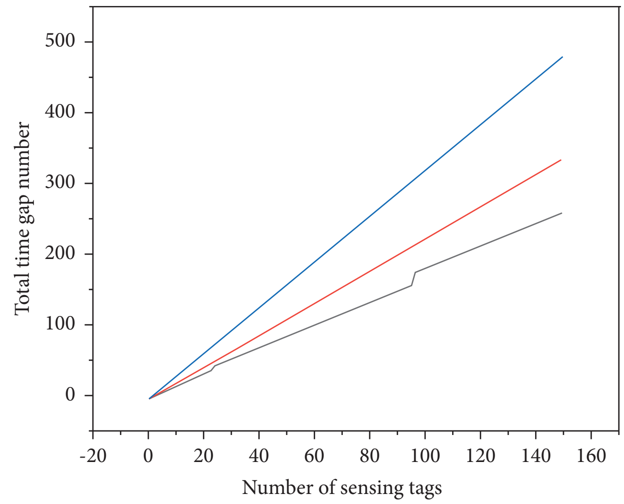

Figure 8: Comparison of total time slots of the algorithm.

4.1.4. Algorithm Simulation and Analysis. From the above analysis, the total time number of the algorithm performance parameters and the total number of transmission times and the calculation speed of the IATMSA algorithm were obtained. The total timing of the IATMSA algorithm is compared with the binary tree algorithm and the collision control tree algorithm, and the modeling results are shown in Figure 8.

Figure 8 shows that the IATMSA algorithm has the lowest total number of times compared to the binary tree algorithm and the collision control tree algorithm. In terms of total time, the IATMSA algorithm is clearly superior to the commonly used binary tree and collision control tree algorithms.

Compare the total number of time slots of IATMSA algorithm, IAMS algorithm, and quadtree algorithm. The simulation results are shown in Figure 9.

As can be seen from Figure 9, with the increase of the number of sensor tags, the total number of time slots of IATMSA algorithm is always smaller than that of IAMS algorithm and quadtree algorithm, basically maintained at 50% to 60%, up to about 75%. The IAMS algorithm is basically about 45%, and the quadtree algorithm is basically about 30%. Because the total number of time slots is the main factor affecting the discrimination delay, IATMSA algorithm is obviously better than IAMS algorithm and quadtree algorithm in discrimination delay. The smaller the discrimination delay, the faster the recognition speed. In addition, the total number of time slots of IATMSA algorithm and IAMS algorithm suddenly changes at a certain point. Because the search depth $k = \log_4 (n_2/3)$ takes a non-negative integer, when k is calculated as a decimal, the system program will take an integer by default, which will lead to $\sum 4^i$ $(i = 0, 1, 2, \ldots, k)$ discontinuity and jump, resulting in mutation of IATMSA algorithm and IAMS algorithm at a certain point.

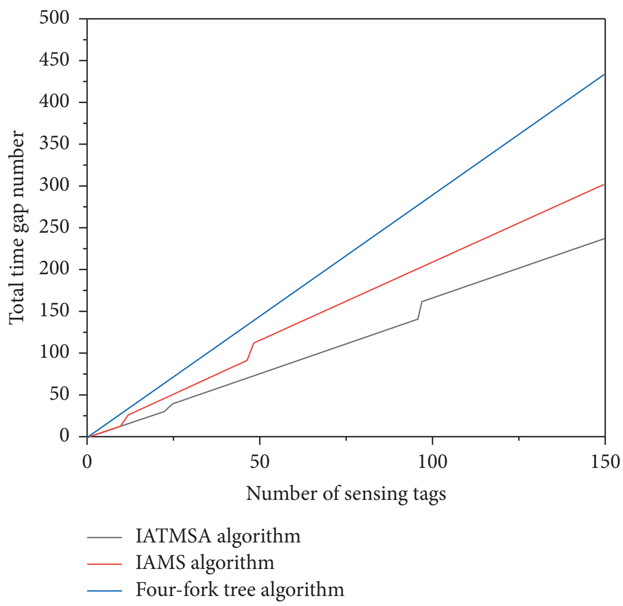

FIGURE 9: Comparison of total time slots of different algorithms.

Based on the fact that the sensor tag in the substation is an active tag, IATMSA algorithm proposes the principle of priority application and allocation of proprietary time slots. For the proprietary time slots that have not applied for collision, the sensor tag can directly and successfully read the status information of electrical equipment, so as to reduce the collision time slots between sensor tags. Based on the established collision probability model, the number of sensor labels applying for collision is determined, and the collision sensor labels are identified by binary tree or quadtree according to IAMS algorithm, so as to obtain the electrical equipment status information of the collision sensor labels. Algorithm simulation results show that the IATMSA algorithm has less total time, higher recognition speeds, and higher transmission speeds compared to the IAMS algorithm and the quadratic algorithm. The IATMSA algorithm can effectively improve the performance of a substation's multiantenna RFID monitoring system.

5. Conclusion

The characteristics of Internet of Things technology meet the communication requirements of building a strong smart grid in China, and it is an area with the most investment in the national Internet of Things investment plan. Currently, as one of the most feasible technologies in power systems, online transmission and conversion equipment control technology is used in most substation equipment, generators, cables, and line insulators of our power system and is the latest technology. Based on the lack of real-time monitoring data, accuracy, and reliability of current power grid monitoring systems, this paper proposes a smart technology study to monitor online green energy transmission and conversion devices based on Internet technology. The sensor tag is integrated with various electrical equipment status monitoring sensors (such as temperature sensor, humidity sensor, acceleration sensor, and vibration sensor), so that the electrical equipment status acquisition terminal has the ability of recognition and perception, and an electrical equipment status monitoring system in the power transmission and transformation environment based on the Internet of Things technology is established.

Aiming at the problem that the signal transmission between reader and sensor tag is affected by multipath effect in substation environment, a solution using multiantenna RFID system is proposed. The channel model of substation multiantenna RFID system is established, compared with the Nakagami-m channel estimation method proposed by predecessors and verified by experiments, and the correctness of the constructed multiantenna RFID system channel is pointed out. Moreover, using the channel model of substation multiantenna RFID system, this paper analyzes the influencing factors of substation multiantenna RFID monitoring system performance in the actual power transmission and transformation environment, and puts forward some installation precautions applied to substation multiantenna RFID monitoring system, so as to provide reference for construction and installation personnel. Finally, based on the collision problem of sensor tags in multiantenna RFID system, a new algorithm is proposed, which is compared with previous algorithms to verify the superiority and practicability of the proposed algorithm, which can effectively improve the performance of substation multiantenna RFID monitoring system.

Data Availability

No data were used to support this study.

Conflicts of Interest

The authors declare that there are no conflicts of interest regarding the publication of this article.

References

[1] X. Ye, Y. Tang, and D. Shu, "Large step size electromagnetic transient simulations by matrix transformation-based shifted-frequency phasor models," *IET Generation, Transmission & Distribution*, vol. 14, no. 15, pp. 2890–2900, 2020.

[2] J. Viljanen, K. Kalmankoski, V. Contreras et al., "Sequential collinear photofragmentation and atomic absorption spectroscopy for online laser monitoring of triatomic metal species," *Sensors*, vol. 20, no. 2, pp. 533–536, 2020.

[3] M. Bernabei, S. Pantalei, and I. Sherrington, "Development of an artificial olfactory system for lubricant degradation monitoring," *International Journal of COMADEM*, vol. 23, no. 1, pp. 3–12, 2020.

[4] J. Meng, M. Singh, M. Sharma, D. Singh, P. Kaur, and R. Kumar, "Online monitoring technology of power transformer based on vibration analysis," *Journal of Intelligent Systems*, vol. 30, no. 1, pp. 554–563, 2021.

[5] Q. Wang and P. Lu, "Research on application of artificial intelligence in computer network technology," *International Journal of Pattern Recognition and Artificial Intelligence*, vol. 33, no. 5, Article ID 1959015, 2019.

[6] L. Zhou, T. Zhang, Z. Zhang, Z. Lei, and S. Zhu, "A new online quality monitoring method of chain resistance upset butt welding based on isolation forest and local outlier factor," *Journal of Manufacturing Processes*, vol. 68, no. 8, pp. 843–851, 2021.

[7] J. Favere, F. Waegenaar, N. Boon, and B. De Gusseme, "Online microbial monitoring of drinking water: how do different techniques respond to contaminations in practice?" *Water Research*, vol. 202, no. 12, pp. 117387–117390, 2021.

[8] K. Guo, "Research on location selection model of distribution network with constrained line constraints based on genetic algorithm," *Neural Computing & Applications*, vol. 32, no. 6, pp. 1679–1689, 2020.

[9] Z. He, L. Xu, J. Mao, X. Han, and B. Zhang, "Application of multistep inversion method for online monitoring aerosol particle size distribution and aerosol concentration," *Mathematical Problems in Engineering*, vol. 2020, no. 8, pp. 1–12, 2020.

[10] Y. Ding, G. Ren, G. Wang et al., "V2o5 nanobelts mimick tandem enzymes to achieve nonenzymatic online monitoring of glucose in living rat brain," *Analytical Chemistry*, vol. 92, no. 6, pp. 4583–4591, 2020.

[11] J. Zhao, D. Wang, F. Zhang, Y. Liu, B. Chen, and Z. L. Wang, "Real-time and online lubricating oil condition monitoring enabled by triboelectric nanogenerator," *ACS Nano*, vol. 15, no. 7, pp. 11869–11879, 2021.

[12] Q. Nazir and C. Shao, "Online tool condition monitoring for ultrasonic metal welding via sensor fusion and machine learning," *Journal of Manufacturing Processes*, vol. 62, no. 5, pp. 806–816, 2021.

[13] H. A. Saeed, H. Wang, M. Peng, A. Hussain, and A. Nawaz, "Online fault monitoring based on deep neural network & sliding window technique," *Progress in Nuclear Energy*, vol. 121, no. 1, pp. 103236–103239, 2020.

[14] K. Mamouras and Z. Wang, "Online signal monitoring with bounded lag," *IEEE Transactions on Computer-Aided Design of Integrated Circuits and Systems*, vol. 39, no. 11, pp. 3868–3880, 2020.

[15] I. Cvitić, D. Peraković, M. Periša, and M. D. Stojanović, "Novel classification of IoT devices based on traffic flow features," *Journal of Organizational and End User Computing*, vol. 33, no. 6, pp. 1–20, 2021.

[16] V. Sathiyamoorthi, P. Keerthika, P. Suresh, A. P. Rao, and K. Logeswaran, "Adaptive fault tolerant resource allocation scheme for cloud computing environments," *Journal of Organizational and End User Computing*, vol. 33, no. 5, pp. 135–152, 2021.

[17] J. D. Pinzon and D. G. Colome, "Pmu-based online monitoring of short-term voltage stability using lyapunov exponents," *IEEE Latin America Transactions*, vol. 17, no. 10, pp. 1578–1587, 2019.

[18] D. Paschalides, D. Stephanidis, A. Andreou et al., "Mandola," *ACM Transactions on Internet Technology*, vol. 20, no. 2, pp. 1–21, 2020.

[19] F. Li, R. Xie, Z. Wang et al., "Online distributed iot security monitoring with multidimensional streaming big data," *IEEE Internet of Things Journal*, vol. 7, no. 5, pp. 4387–4394, 2020.

[20] T. Kambayashi, T. Noguchi, A. Nojima, S. Kono, S.-i. Taniguchi, and Y. Ozaki, "Glucose monitoring in cell culture with online ultrasound-assisted near-infrared spectroscopy," *Analytical Chemistry*, vol. 92, no. 4, pp. 2946–2952, 2020.

[21] Y. Zhang, H. G. Soon, D. Ye, J. Y. H. Fuh, and K. Zhu, "Powder-bed fusion process monitoring by machine vision with hybrid convolutional neural networks," *IEEE Transactions on Industrial Informatics*, vol. 16, no. 9, pp. 5769–5779, 2020.

[22] S. Kim, M. K. M. Jeong, and E. A. Elsayed, "A penalized likelihood-based quality monitoring via L2-norm regularization for high-dimensional processes," *Journal of Quality Technology*, vol. 52, no. 3, pp. 265–280, 2020.

[23] R. Dindorf and P. Wos, "Universal programmable portable measurement device for diagnostics and monitoring of industrial fluid power systems," *Sensors*, vol. 21, no. 10, pp. 3440–3443, 2021.

[24] X. Yuan, Y. He, S. Wan, M. Qiu, and H. Jiang, "Remote vibration monitoring and fault diagnosis system of synchronous motor based on internet of things technology," *Mobile Information Systems*, vol. 2021, no. 2, pp. 1–10, 2021.

[25] J.-C. Fan-Jiang, C.-W. Su, G.-Y. Liou et al., "Study of an online monitoring adaptive system for an injection molding process based on a nozzle pressure curve," *Polymers*, vol. 13, no. 4, pp. 555–559, 2021.